JOURNAL OF MATERIALS SCIENCE 26 (1991) 3955–3963

# Mechanism of order-induced embrittlement in Ni–$Ni_4Mo$ alloys

H. M. TAWANCY
*Materials Characterization Laboratory, Metrology, Standards and Materials Division, Research Institute, King Fahd University of Petroleum and Minerals, PO Box 1639, Dhahran 31261, Saudi Arabia*

Intergranular embrittlement of Ni–Mo alloys by long-range ordering to $Ni_4Mo$ was examined for an off-stoichiometric alloy and a stoichiometric alloy of known impurity contents. Both tensile properties and corrosion resistance in HCl were measured as functions of exposure time at 700 °C. Various techniques employed for microstructural characterization and microchemical analysis included analytical electron microscopy, X-ray diffractometry and Auger electron spectroscopy. During exposure at 700 °C, the yield-strength maxima in both alloys were reached before the ductility minima. Homogeneous matrix ordering was observed to cause a moderate loss of ductility and the fracture mode remained to be transgranular. However, a considerable loss of ductility, intergranular embrittlement and extensive intergranular corrosion attack were found to be associated with heterogeneous grain-boundary ordering, which occurred by a discontinuous mechanism. Discontinuous ordering resulted in molybdenum-depleted zones alongside grain boundaries as evinced from microchemical analysis and localized corrosion attack. It was concluded that the observed intergranular embrittlement was caused by highly localized deformation in the molybdenum-depleted zones.

## 1. Introduction

Structural applications of ordered alloys and intermetallic compounds are generally limited by their relatively low ductility [1]. Recently, however, a considerable progress has been made toward ductilizing many intermetallic compounds, e.g. $Ni_3Al$ [2, 3]. Among the nickel-base alloys embrittled by long-range ordering are those containing 26–28 wt % Mo [4–6]. Due to their outstanding corrosion resistance in reducing media, these alloys have been of particular importance to the chemical process industry [7]. Typically, in the solution heat-treated condition (f.c.c. solid solution), the alloy contains short-range order [8, 9]. Long-range order to $Ni_4Mo$ (tetragonal, $D1_a$ superlattice), occurs upon exposure to temperatures in the range of 600–800 °C.

Similar to the case of $Ni_3Al$, a single crystal of $Ni_4Mo$ is highly ductile [10]. However, a polycrystalline ordered alloy becomes extremely brittle [4–6]. In this condition, tensile fracture occurs exclusively along the grain boundaries of the parent disordered phase [4. 11]. Such behaviour indicates that the embrittlement might be related to a grain-boundary effect. It has been suggested that the embrittlement of a stoichiometric $Ni_4Mo$ alloy (Ni–29.1 wt % Mo) could be due to the coarse recrystallized structure which develops at grain boundaries after extended exposure at a given temperature [12]. In another study, however, tensile property data derived from a stoichiometric alloy indicates that the embrittlement is observed prior to the development of the grain-boundary structure [6].

Generally, ordered alloys and intermetallic compounds are known to be embrittled by two mechanisms [13]: (a) restriction of slip and/or cross-slip systems due to long-range ordering, and (b) grain-boundary hardening due to impurity segregation. Nickel-base alloys, in particular, can be embrittled by sulphur segregation to grain boundaries [13]. Since the impurity contents of the alloys utilized in the above studies were not specified, it is rather difficult to separate any possible contribution of impurity segregation to embrittlement, from that due to ordering. Another complication which arises in the case of Ni–Mo alloys is the effect of small concentrations of Cr and Fe which can significantly influence the ordering behaviour [8]. Thus, it is possible that the exact mechanism responsible for the embrittlement is a sensitive function of chemical composition.

Development of ductile ordered alloys and intermetallic compounds for structural applications requires a basic understanding of the embrittlement mechanism. For example, in the case of $Co_3V$, it has been determined that its embrittlement is caused by the characteristic hexagonal stacking sequence which is related to the electron density ratio [14]. By substituting Ni and Fe for Co, it was possible to lower the electron density ratio to the level which favours a cubic stacking sequence and, in turn, an improved ductility. Toward that objective, the present investigation was undertaken to determine the mechanism responsible for embrittling an off-stoichiometric alloy and a stoichiometric $Ni_4Mo$ alloy of known impurity contents.

0022–2461/91 $03.00 + .12 

TABLE I Chemical compositions of the alloys investigated (wt %)

| Element | Off-stoichiometric | Stoichiometric |
|---|---|---|
| Ni | Balance | Balance |
| Mo | 26.92 | 29.12 |
| Fe | 0.93 | < 0.1 |
| Cr | 0.64 | < 0.1 |
| P | 0.01 | 0.01 |
| C | 0.002 | 0.002 |
| S | < 0.002 | < 0.002 |

## 2. Experimental procedure

Alloys investigated were prepared by vacuum melting and then processed into 1 mm thick sheets. Table I summarizes their chemical compositions. Specimens were solution heat-treated at 1065 °C for 15 min and then water-quenched. Subsequently, they were exposed at 700 °C for up to 1000 h to induce long-range ordering.

Both room-temperature tensile properties and corrosion rates in boiling 20% HCl were measured as functions of exposure time at 700 °C. All tensile tests were conducted on specimens having a gauge length of 50.8 mm. Corrosion rates were calculated from weight loss measurements made on 25.4 mm × 25.4 mm × 1 mm specimens after 24 h immersion in HCl. It is to be noted that the reducing acid test highlights regions which are depleted in Mo [7]. Fractography was conducted in a scanning electron microscope (SEM). For certain exposure conditions where the fracture mode was determined by SEM to be predominantly intergranular, selected specimens were fractured *in situ* in a scanning Auger microprobe and the chemical compositions of freshly exposed grain boundaries were analysed. Also, molybdenum–depth profiles were generated by sputtering thin layers at a rate of 1 nm $min^{-1}$.

Microstructural characterization was conducted in the transmission electron microscopy (TEM) and scanning transmission electron microscopy (STEM) modes of an analytical electron microscope operating at 200 kV. Thin foils were prepared by the jet polishing technique in a solution consisting of 30% nitric acid in methanol kept at about − 20 °C. Both electron and X-ray diffraction were utilized to characterize the nature of ordered phases. X-ray diffractometry was conducted on as-polished specimens. These specimens were subsequently etched in a solution consisting of 80% HCl and 20% of 15 mol % chromic acid for light-optical metallography work.

## 3. Results and discussion

### 3.1. Effect of ordering on tensile properties and microstructure

Fig. 1 illustrates the effect of up to 1000 h of exposure at 700 °C on the room-temperature tensile properties of the alloys investigated. For the stoichiometric alloy, the yield strength can be seen to reach its maximum value within the first 15 min of exposure. At the onset of maximum yield strength, however, a tensile elongation of 32% was maintained.

Although with continued exposure up to 1000 h the yield strength remained nearly unchanged, the tensile elongation was observed to considerably decrease until complete loss of ductility occurred after about 1 h. Qualitatively, a similar behaviour was observed for the off-stoichiometric alloy where a tensile elongation of 44% was maintained at the onset of maximum yield strength after about 1 h of exposure at 700 °C.

As can be seen from Fig. 1, the changes in tensile properties of the off-stoichiometric alloy lagged behind those of the stoichiometric alloy. Such a difference in behaviour could be explained in terms of the effect of Mo concentration on the ordering kinetics. As the stoichiometric composition is approached, the establishment of $Ni_4Mo$ composition becomes less dependent on long-range diffusion of Mo. Consequently, the ordering kinetics in the off-stoichiometric alloy would be expected to be more sluggish as compared to the stoichiometric alloy. Although both alloys reached the same level of tensile ductility after about 24 h of exposure, the maximum yield strength of the off-stoichiometric alloy was markedly less. Such behaviour could be attributed to the smaller volume fraction of $Ni_4Mo$ in the matrix of the off-stoichiometric alloy.

It could be concluded from the tensile data of Fig. 1 that for the alloys investigated, the yield strength maxima were reached before the ductility minima during exposure at 700 °C. Since the increase in yield strength is primarily determined by matrix ordering, the considerable loss of ductility encountered in the later stages of exposure appeared to be related to some other effect. Qualitatively, the microstructures of the two alloys were found to be similar. To avoid repetition, only the microstructures derived from the off-stoichiometric alloy are presented below.

Similar to the case of other ordered alloys such as $Ni_3Fe$, $Ni_2V$ and $Ni_2Cr$ [15], long-range ordering to $Ni_4Mo$ was observed to occur homogeneously in the matrix and heterogeneously at grain boundaries [4]. For example, Fig. 2 illustrates the effect of 100 h of exposure at 700 °C on the gross microstructural features of the off-stoichiometric alloy. Table II summarizes the result of phase analysis of X-ray diffractometry corresponding to the microstructure of Fig. 2b. Two phases were identified, namely $Ni_4Mo$ and retained disordered phase. A similar result was obtained by electron diffraction. Quantification of the X-ray diffraction data revealed that the volume fraction of $Ni_4Mo$ was $\sim 0.75$. For the stoichiometric alloy, the volume fraction of $Ni_4Mo$ was determined to be about 98%. As can be seen from Fig. 2, $Ni_4Mo$ assumed two distinct morphologies: (a) Widmanstatten-type in the matrix, and (b) lamellar at the grain boundaries. Corresponding features of the two morphologies on the finer scale of TEM are illustrated in Fig. 3. Similar to other Ni–Mo alloys [16], the Widmanstatten pattern consisted of twin-related crystals along the {1 0 0} planes of the tetragonal $D1_a$ superlattice. A lamellar morphology such as that shown in Figs 2b and 3b is typical of a discontinuous grain-boundary reaction.

At the onset of maximum yield strength during exposure at 700 °C, both alloys were found to deform

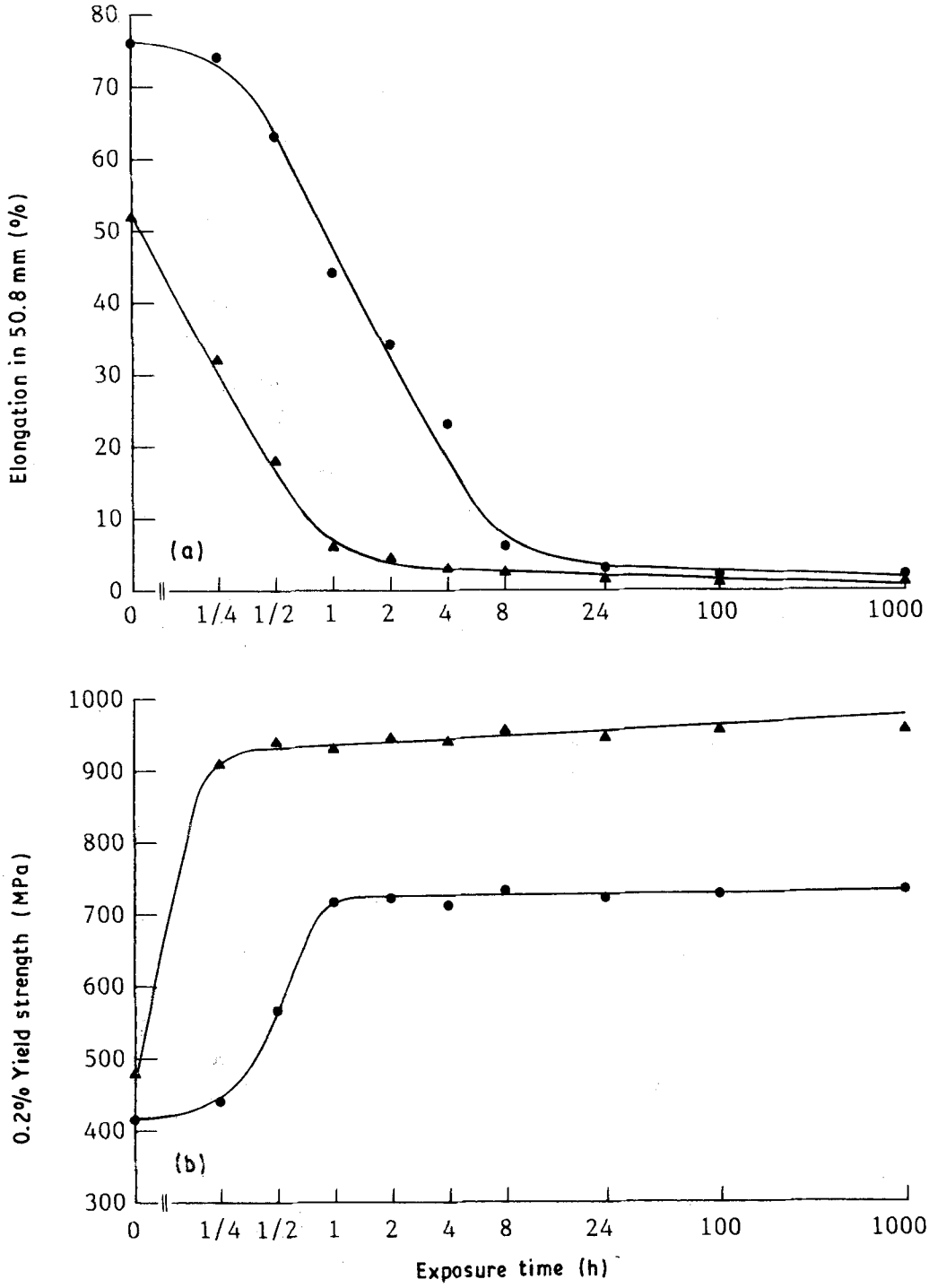


*Figure 1* Effect of exposure time at 700 °C on the room-temperature tensile properties of (●) the off-stoichiometric alloy and (▲) the stoichiometric alloy (for compositions see Table I): (a) elongation, (b) yield strength.

predominantly by twinning on the {1 1 1} planes of the parent disordered f.c.c. phase. An example is shown in Fig. 4 for a specimen of the off-stoichiometric alloy given 20% elongation after 1 h exposure at 700 °C. The corresponding tensile ductility was 44%. Ordered $Ni_4Mo$ domains observed within the deformation twins demonstrated that twinning could occur without disrupting the atomic order. From a consideration of the crystallography of $A_4 \rightarrow D1_a$ transformation, it can readily be shown that deformation by twinning is energetically favourable in the ordered state [17]. At this stage, the ordering mechanism was found to be of the homogeneous type within the matrix and fracture occurred transgranularly as shown later in this section. It could thus be concluded that homogeneous matrix ordering results in a moderate loss of ductility, which is consistent with the observation that a single crystal of $Ni_4Mo$ is highly ductile.

When the lamellar structure was formed at grain boundaries during the later stages of exposure, a high density of $\{1\,1\,1\}_{f.c.c.}$ stacking faults was observed in the deformation substructure. An example is illustrated in Fig. 5 for a specimen exposed for 100 h at 700 °C and then given 2% elongation. In this case, the corresponding tensile ductility was only 3% and the fracture mode was predominantly intergranular. Overlapped stacking-fault contrast observed in Fig. 5 is character-

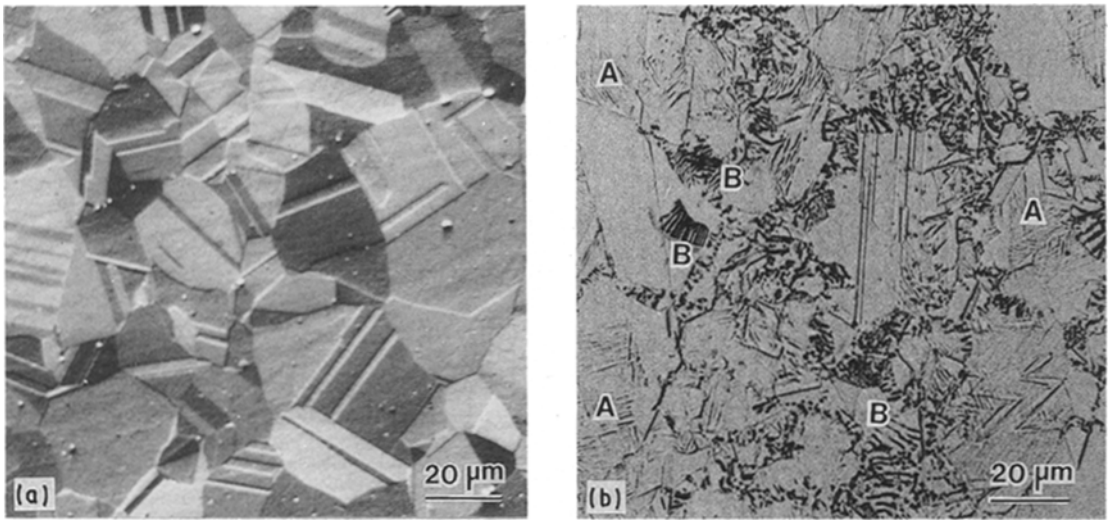


*Figure 2* Effect of 100 h exposure at 700 °C on the gross microstructural features of the off-stoichiometric alloy: (a) annealed condition (secondary electron SEM image); (b) after 100 h exposure (light-optical micrograph).

TABLE II X-ray diffractometer data derived from the off-stoichiometric alloy (exposed 1–1000 h at 700 °C)

| (*h k l*) | Phase | *d*-spacing (nm) | |
|---|---|---|---|
| | | Observed | Calculated |
| (1 1 0) | $Ni_4Mo$: | 0.4051 | 0.4049 |
| (1 0 1) | tetragonal, | 0.3035 | 0.3027 |
| (2 0 0) | $a = 0.5727$ nm, | 0.2870 | 0.2863 |
| (3 1 0) | $c = 0.3566$ nm | 0.1817 | 0.1811 |
| (0 0 2) | | 0.1787 | 0.1783 |
| (1 1 2) | | 0.1651 | 0.1632 |
| (2 0 2) | | 0.1520 | 0.1514 |
| (3 2 1) | | 0.1462 | 0.1451 |
| (1 1 1) | f.c.c. phase, | 0.2080 | 0.2078 |
| (2 0 0) | $a = 0.360$ nm | 0.1805 | 0.1800 |
| (2 2 0) | | 0.1276 | 0.1273 |

istic of alloys with a high tendency to twin and, thus, is representative of an early stage of twinning. It could be concluded from this observation that in the presence of the lamellar grain-boundary structure, fracture had occurred before the faults could grow into twins.

Fig. 6 illustrates typical tensile fracture surfaces of the off-stoichiometric alloy in the following conditions: (a) annealed (disordered, 76% tensile ductility), (b) exposed 1 h at 700 °C (homogeneously ordered, 44% tensile ductility), and (c) exposed 100 h at 700 °C (homogeneously and heterogeneously ordered, 3% tensile ductility). As expected, in the disordered state fracture occurred transgranularly by microvoid coalescence (dimple-type rupture), as shown in Fig. 6a. When the alloy was homogeneously ordered, fracture proceeded by the same mechanism; however, the size of dimples can be seen to become comparatively finer (Fig. 6b). This suggested a higher density of fracture initiation sites, e.g. intersections of twins. Corresponding to the condition of homogeneous and heterogeneous grain-boundary ordering, the fracture mode was found to be predominantly intergranular as illustrated in Fig. 6c. A behaviour similar to that described above was observed for the stoichiometric alloy.

To summarize, the tensile and fracture behaviour of the alloys investigated appeared to be sensitive functions of the ordering mechanism. When homogeneous matrix ordering prevailed in the early stages of exposure, a relatively high ductility level was maintained and the fracture mode was transgranular. However, a considerable loss of ductility and intergranular

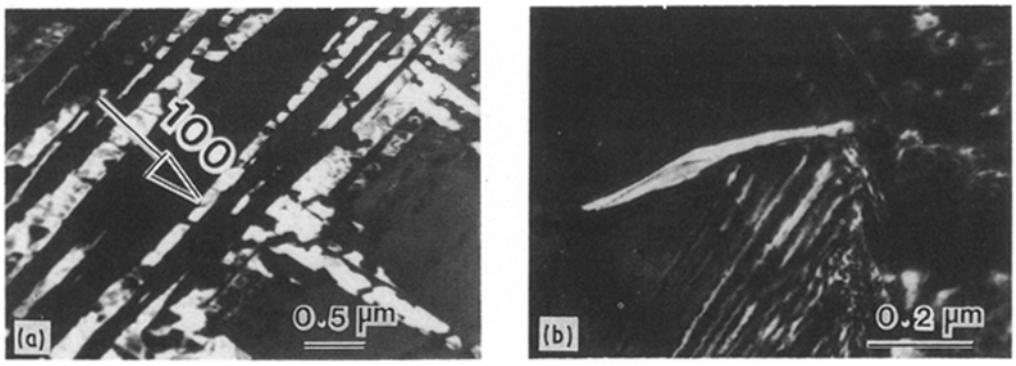


*Figure 3* Dark-field TEM images formed with 1/5 $\langle 4\,2\,0 \rangle_{f.c.c.}$ superlattice reflections to illustrate the morphological features of homogeneous matrix ordering and heterogeneous grain-boundary ordering in the off-stoichiometric alloy after 100 h exposure at 700 °C: (a) mosaic assembly of $\{1\,0\,0\}_{tetragonal}$ transformation twins formed by homogeneous matrix ordering; (b) an $Ni_4Mo$ lamella formed at a grain boundary by heterogeneous ordering.

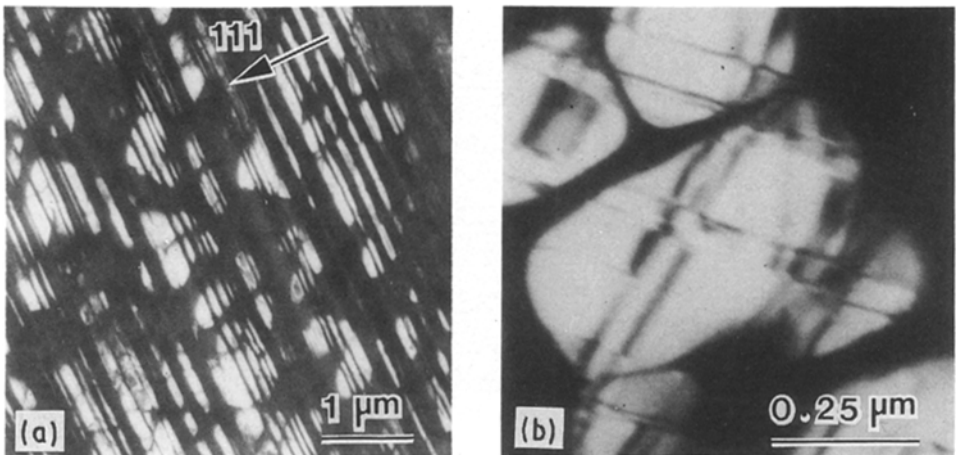


*Figure 4* Dark-field TEM images illustrating the deformation substructure in a specimen of the off-stoichiometric alloy given 20% tensile elongation at room temperature after 1 h exposure at 700 °C: (a) a dark-field image formed with a twin reflection to illustrate $\{1\,1\,1\}_{f.c.c.}$ deformation twins; (b) a dark-field image formed with a $1/5\ \langle 4\,2\,0\rangle_{f.c.c.}$ superlattice reflection to illustrate $Ni_4Mo$ domains within the twins.

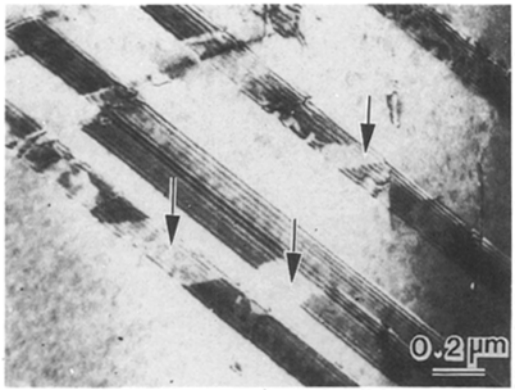


*Figure 5* Bright-field TEM image illustrating a high density of stacking faults in a specimen of the off-stoichiometric alloy given 2% tensile elongation at room temperature after 100 h exposure at 700 °C. Overlapped stacking faults are indicated by the arrows.

embrittlement were experienced due to heterogeneous grain-boundary ordering which occurred at the later stages of exposure. To further clarify the mechanism by which the alloy is embrittled, the chemical compositions of embrittled grain boundaries were characterized as described below.

## 3.2. Influence of ordering on grain-boundary chemistry

Fig. 7 summarizes the results of Auger analysis of grain boundaries in specimens of the off-stoichiometric alloy after 100 h exposure at 700 °C. Under these conditions the alloy was homogeneously and heterogeneously ordered (Fig. 2b), and the tensile fracture mode was predominantly intergranular as shown in Fig. 6c. By comparing the Auger spectra of Fig. 7a and b which were derived from a freshly exposed boundary and after sputtering a 24 nm thick layer, respectively, it could be concluded that the grain boundary was considerably depleted in Mo. Fig. 7c shows a molybdenum–depth profile which illustrates the concentration of Mo as a function of distance from a grain boundary. At a distance of about 9 nm from the grain boundary, the Mo concentration reached the level typical of the alloy. Another important feature derived from Fig. 7a and b was the absence of impurity segregation at grain boundaries, particularly S and P. Thus, it could be concluded that impurity segregation to grain boundaries had played no role in the observed embrittlement of the alloys investigated.

Another example demonstrating the Mo depletion alongside grain boundaries is given in the STEM analysis of Fig. 8. It illustrates the result of microchemical analysis of the $Ni_4Mo$ lamella and the adjacent matrix of Fig. 3b using a 2 nm probe diameter at 200 kV. As can be seen, the results were consistent with those of the Auger analysis described above.

Depletion of Mo alongside grain boundaries in the heterogeneously ordered state was also reflected by corrosion tests in boiling 20% HCl. A one-to-one correspondence between the decrease in tensile ductility and increase in corrosion rate was observed during exposure at 700 °C as shown in Fig. 9. Similar to the case of tensile ductility, a considerable increase in the corrosion rate occurred in the later stages of exposure when the lamellar structure was formed at grain boundaries. Fig. 10 compares the microstructures of corrosion-tested specimens in the annealed condition and after 100 h exposure at 700 °C. Although the corrosion attack was observed to be uniform in the annealed condition (general thinning) as shown in Fig. 10a, extensive intergranular attack occurred in the exposed condition (Fig. 10b). As pointed out earlier, the reducing acid test highlights regions which are molybdenum-depleted. Since no carbide precipitates were observed at grain boundaries, it was concluded that the observed intergranular attack was due to the Mo depletion associated with heterogeneous ordering.

## 3.3. Embrittlement mechanism

It is well known that when a supersaturated solid solution decomposes by a discontinuous mechanism at grain boundaries, it results in a matrix phase depleted in solute element [18]. In the present case, the

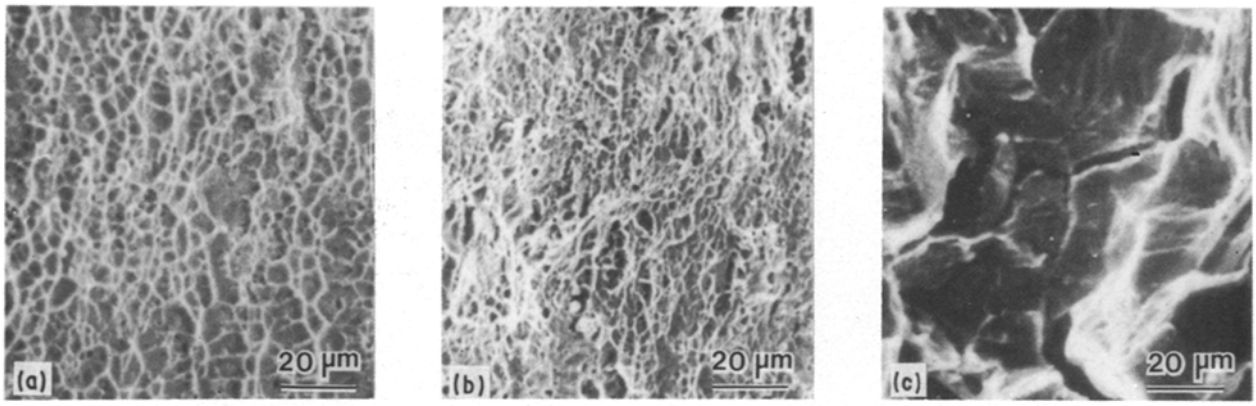


*Figure 6* Effect of exposure time at 700 °C on the tensile fracture mode of the off-stoichiometric alloy (secondary electron SEM images): (a) unexposed (annealed), (b) exposed 1 h at 700 °C, (c) exposed 100 h at 700 °C.

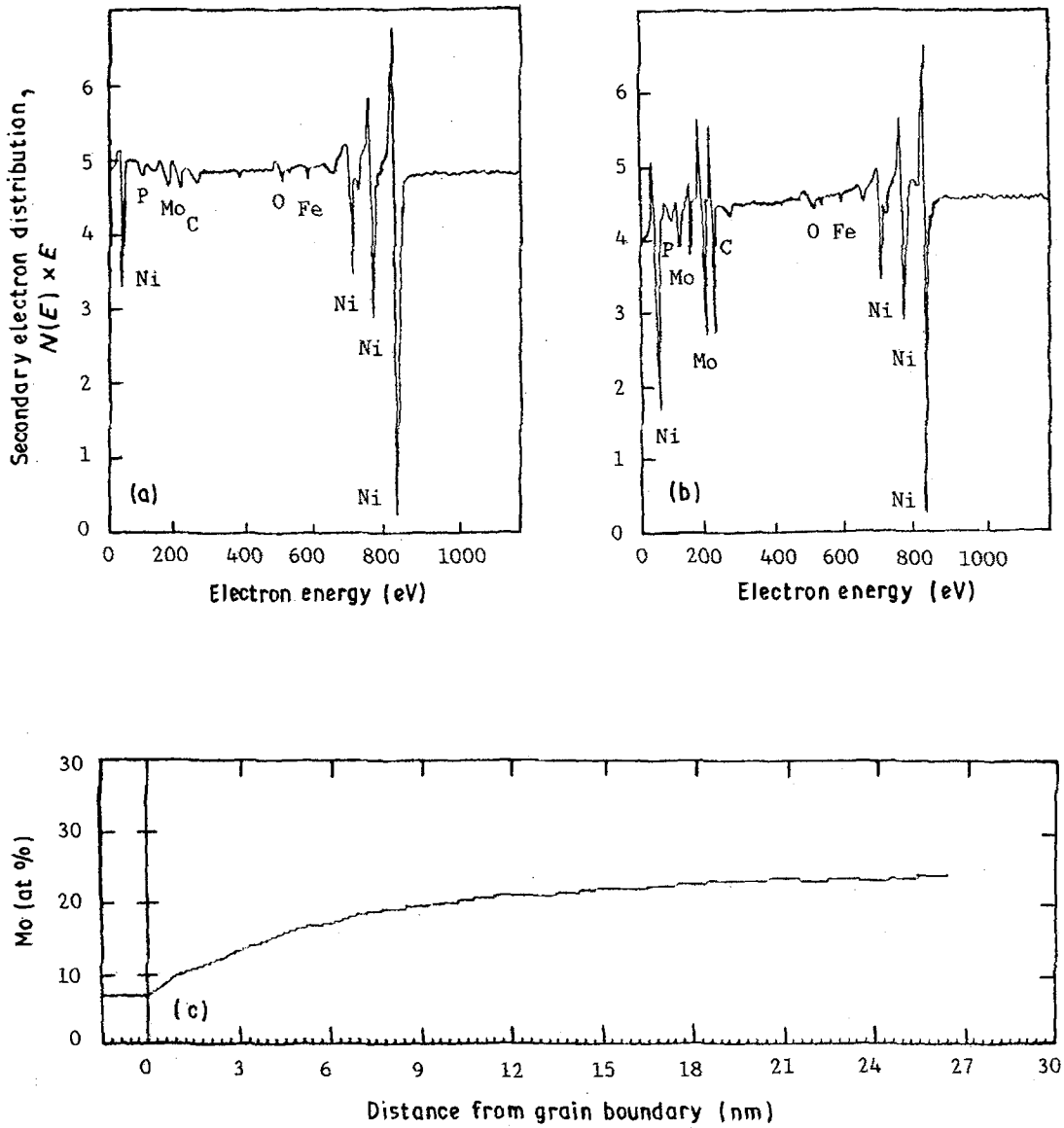


*Figure 7* Auger analysis of grain boundaries in the off-stoichiometric alloy after 100 h exposure at 700 °C: (a) Auger spectrum derived from a grain boundary in the as-fractured condition; (b) Auger spectrum derived from the same region of (a) after sputtering a 24 nm thick layer; (c) molybdenum–depth profile illustrating the concentration of Mo as a function of distance from a grain boundary.

resulting matrix becomes depleted in Mo. Due to the very slow diffusivity of Mo in Ni, re-establishment of equilibrium conditions at grain boundaries can be expected to be extremely sluggish. Consequently, relatively "soft" zones are created alongside grain boundaries where plastic deformation can become highly localized.

In view of the observed relatively small concentration of Mo alongside grain boundaries, these relatively "soft" zones can be expected to deform by slip, and

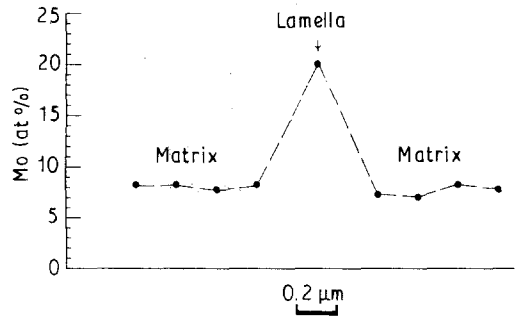


*Figure 8* Result of STEM microchemical analysis of Mo concentration in the $Ni_4Mo$ lamella and adjacent matrix of Fig. 3b using a 2 nm probe diameter at 200 kV.

thus strain-harden at a considerably faster rate as compared to the matrix which was shown to deform by twinning. It is then possible that heterogeneous grain-boundary ordering leads to initiation of intergranular fracture before the matrix deforms by twinning. This is consistent with the observation of Fig. 5. Closer examinations of tensile fracture surfaces revealed highly localized deformation near grain boundaries which was indicative of alloy depletion. An example is given in Fig. 11 for the off-stoichiometric alloy after 100 h exposure at 700 °C. Separated-grain facets are observed in Fig. 11a. However, dimples can be distinguished on a portion of one facet in Fig. 11b which is characteristic of microvoid coalescence in the grain-boundary zone. This feature is typical of alloy depletion at grain boundaries.

## 4. Conclusions

The mechanism of order-induced embrittlement was examined in an off-stoichiometric alloy and a stoichiometric $Ni_4Mo$ alloy. Ordering in both alloys was found to occur homogeneously in the matrix and

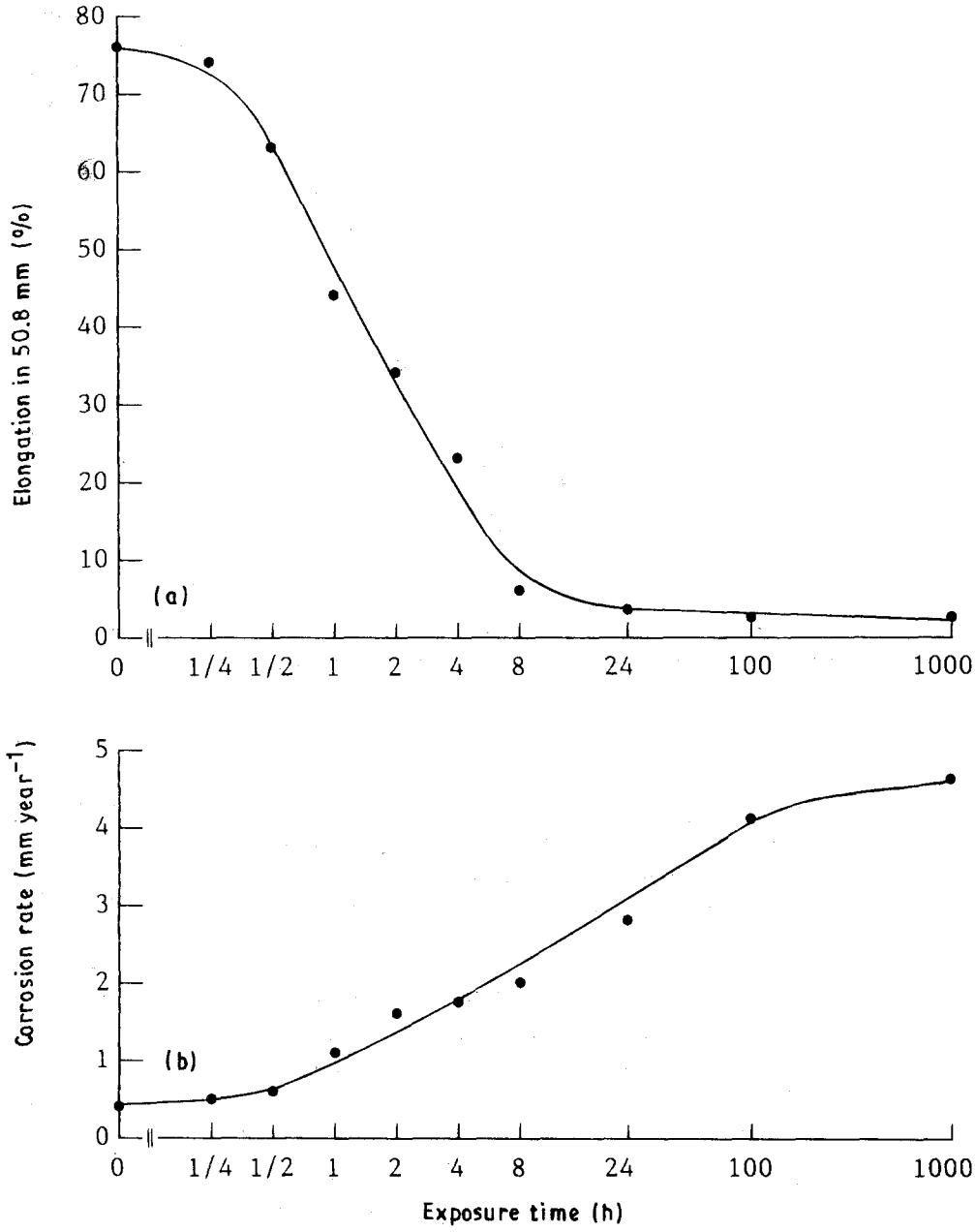


*Figure 9* Comparative effect of exposure time at 700 °C on (a) the room-temperature tensile ductility and (b) the corrosion rate in boiling 20% HCl of the off-stoichiometric alloy.

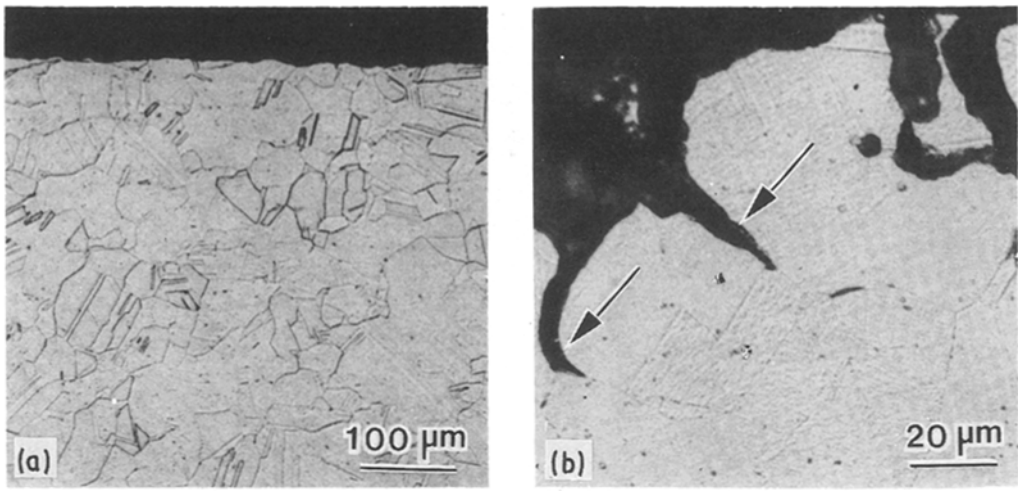


*Figure 10* Light-optical micrographs illustrating comparative microstructural features of specimens of the off-stoichiometric alloy after corrosion testing in boiling 20% HCl: (a) annealed (unexposed), (b) after 100 h exposure at 700 °C; intergranular corrosion attack is indicated by the arrows.

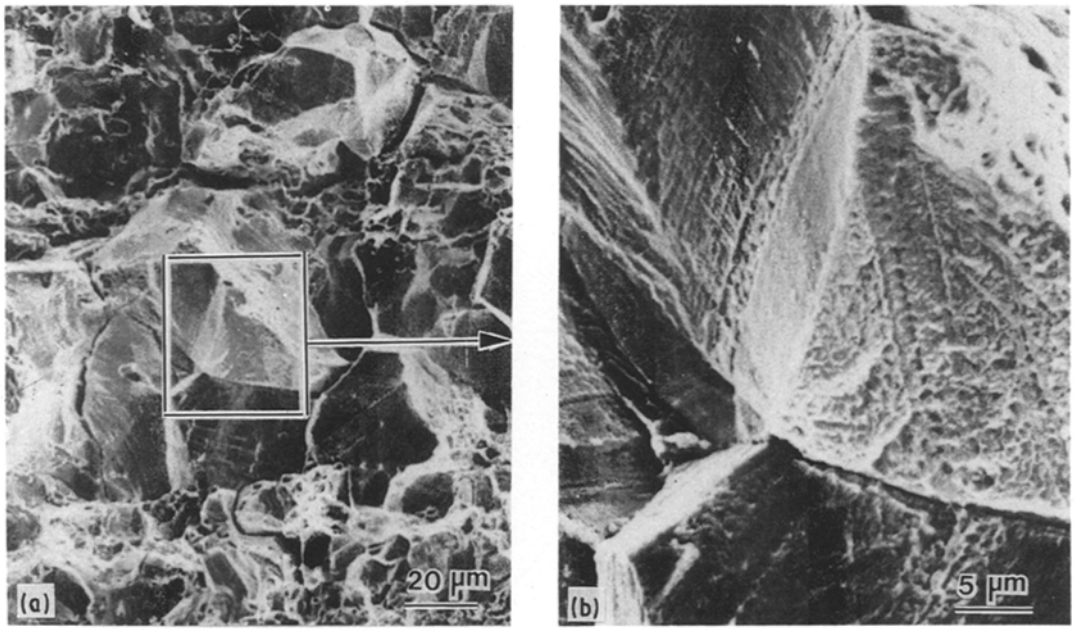


*Figure 11* Secondary-electron SEM images illustrating a characteristic tensile fracture surface of a specimen of the off-stoichiometric alloy after 100 h exposure at 700 °C: (a) separated-grain facets, (b) dimples on the enclosed facet in (a).

heterogeneously at grain boundaries by a discontinuous mechanism. Homogeneous matrix ordering was found to result in a moderate loss of ductility. In contrast, a considerable loss of ductility was associated with heterogeneous grain-boundary ordering. It was determined that discontinuous ordering results in molybdenum-depleted zones alongside grain boundaries. Highly localized deformation in these relatively "soft" zones was found to promote intergranular embrittlement.

## Acknowledgements

The support of the Research Institute, King Fahd University of Petroleum and Minerals, and permission to publish this work are greatly appreciated.

## References

1. N. S. STOLOFF, *Int. Met. Rev.* **29**(3) (1984) 123.
2. C. T. LIU, C. L. WHITE and J. A. HORTON, *Acta Metall.* **33**(20) (1985) 213.
3. C. T. LIU, C. L. WHITE, C. C. KOCH and E. H. LEE, in Proceedings of Symposium on High Temperature Materials Chemistry-II, edited by Z. A. Munir and D. Cubicciotti (Electrochemical Society, Vol. 83, No. 7, Princeton, New Jersey, 1983) p. 32.
4. H. M. TAWANCY and N. M. ABBAS, *J. Mater. Sci.* **24** (1989) 1845.
5. H. M. TAWANCY and A. I. ASPHAHANI, in "High Temperature Ordered Alloys and Intermetallic Compounds", Vol. 39, edited by C. C. Koch, C. T. Liu and N. S. Stoloff (Materials Research Society, Boston, 1985) p. 455.
6. C. R. BROOKS, J. E. SPRUIELL and E. E. STANSBURY, *Int. Met. Rev.* **29**(3) (1984) 210.
7. F. G. HODGE and R. W. KIRCHNER, *Mater. Performance* **15** (1976) 40.

8. H. M. TAWANCY and M. O. ABOELFOTOH, *Phys. Status Solidi (a)* **99** (1987) 461.
9. H. M. TAWANCY, *Scripta Metall.* **18** (1984) 343.
10. G. I. NOSOVA and N. A. POLYAKOVA, *Phys. Met. Metallogr.* **39**(4) (1975) 140.
11. W. B. SNYDER and C. R. BROOKS, in "Ordered Alloys", edited by B. H. Kear, C. T. Sims and N. S. Stoloff (Claitor's, Baton Rouge, 1970) p. 275.
12. B. CHAKRAVVARTI, E. A. STRAKE and B. G. LeFEVRE, *J. Mater. Sci.* **5** (1970) 394.
13. N. S. STOLOFF and R. G. DAVIES, *Progr. Mater. Sci.* **13**(1) (1966) 3.
14. C. T. LIU, *Int. Met. Rev.* **29**(3) (1984) 168.
15. L. E. TANNER and H. J. LEAMY, in "Order-Disorder Transformations in Alloys", edited by H. Warlimont (Springer, New York, 1974) p. 180.
16. E. RUEDL, P. DELAVIGNETTE and S. AMELINCKX, *Phys. Status Solidi* **28** (1968) 305.
17. L. A. NESBIT and D. E. LAUGHLIN, *Acta Metall.* **28** (1980) 989.
18. D. B. WILLIAMS and E. P. BUTLER, *Int. Met. Rev.* **26**(3) (1981) 153.

*Received 20 June*
*and accepted 26 June 1990*